Journal of African Earth Sciences 102 (2015) 166–179

Contents lists available at ScienceDirect

Journal of African Earth Sciences

journal homepage: www.elsevier.com/locate/jafrearsci

Geochemistry and geochronology of granitoids in the Kibi-Asamankese area of the Kibi-Winneba volcanic belt, southern Ghana

Solomon Anum [a,*], Patrick Asamoah Sakyi [b], Ben-Xun Su [c], Prosper M. Nude [b], Frank Nyame [b], Daniel Asiedu [b], Daniel Kwayisi [b]

[a] Geological Survey Department, P.O. Box KF 672, Koforidua, Ghana
[b] Department of Earth Science, University of Ghana, P.O. Box LG 58, Legon-Accra, Ghana
[c] State Key Laboratory of Lithospheric Evolution, Institute of Geology and Geophysics, Chinese Academy of Sciences, P.O. Box 9825, Beijing 100029, China

ARTICLE INFO

Article history:
Received 28 May 2014
Received in revised form 15 November 2014
Accepted 18 November 2014
Available online 27 November 2014

Keywords:
Granitoids
Geochronology
West African Craton
Birimian
Asamankese
Ghana

ABSTRACT

In Ghana the West African Craton is represented by Birimian and Tarkwaian rocks with extensive granitoid bodies. Granitoids from Asamankese area of the Kibi-Winneba volcanic belt, southern Ghana were analysed for major and trace element contents and found to be characterised by highly-fractionated REE, enrichments, in LILE, and depletion in Nb, Ta and Sr. The LILE enrichment relative to strong Nb–Ta depression, indicates that these granitoids were emplaced in an active margin. Based on field relations, geochemical composition and geochronological data, the granitoids from the Kibi-Asamankese area can be divided into three types, namely; the Eburnean biotite granodiorite (2133–2127 Ma) and hornblende granodiorite (2147 Ma), and the Pre-Eburnean gneissic biotite granite (2193 Ma). The geochemical data of the studied rocks plot in the tholeiitic field, whereas on the A/CNK–A/NK diagram, they generally fall within the metaluminous field, with A/CNK values between 0.69 and 0.88. U–Pb dating of zircons in the granitoids yielded ages ranging from 2193 to 2127 Ma, which are among the oldest ages obtained from the granitoid plutons in Ghana. Such high-precision geochronological data indicate that magmatism occurred over a time-span of about 70 Ma. This provides further evidence that the period 2.1–2.2 Ga was one of the important stages of Birimian magmatism that led to the generation of the granitoids. From the above-mentioned ages, it is possible to link the geological activities to crustal processes and establish the cyclic geotectonic evolution in the West African Craton over time as part of an arc-back-arc basin system.

1. Introduction

Paleoproterozoic rocks, which comprise the bulk of the Birimian terrane of the Leo-Man shield, form a significant portion of the West African Craton (WAC) to the east and north of the Archean Liberian cratonic nucleus (Fig. 1).

The Paleoproterozoic terrane is characterised by narrow sedimentary basins and linear, arcuate volcanic belts and intruded by several generations of granitoids (Leube et al., 1990; Hirdes et al., 1996; Doumbia et al., 1998), and corresponds to a period of accretion during the 2.1–2.0 Ga Eburnean orogeny (e.g., Abouchami et al., 1990). Available data suggest that much of Western Africa is underlain by a crust formed during the Eburnean orogeny at about 2.1 Ga ago (Taylor et al., 1988; Abouchami et al., 1990), a time that has generally been considered to be related to one of relatively slow crustal growth stages, intervening between two well-documented geochronological peaks at approximately 2.6–2.8 Ga and 1.6–1.9 Ga.

The Eburnean tectono-thermal event was accompanied by the deformation and the emplacement of syn- to post-orogenic tonalite–trondhjemite–granodiorite (TTG) and granite plutons along fractures (e.g., Leube et al., 1990; Vidal and Alric, 1994; Feybesse et al., 2006). The event resulted in widespread metamorphism mostly under greenschist-facies conditions (e.g., Oberthür et al., 1996; Béziat et al., 2000). Also, evidence of medium amphibolite-facies metamorphism may be observed in the vicinity of granitoid plutons (e.g., Junner, 1940; Eisenlohr and Hirdes, 1992; Debat et al., 2003).

In Ghana, the Paleoproterozoic supracrustal rocks are subdivided into the Birimian and Tarkwaian. The Birimian is mainly characterised by a series of sub-parallel, roughly equal-spaced northeast–southwest trending volcanic belts with intervening basins, both of which are intruded by extensive granitoids of Proterozoic age. Leube et al. (1990) suggested that these composite belts were predominantly volcano-plutonic ridges which

* Corresponding author. Tel.: +233 (0)242988847.
E-mail address: anumsolo@yahoo.com (S. Anum).

http://dx.doi.org/10.1016/j.jafrearsci.2014.11.007
1464-343X/

generated coeval sediments through in situ stripping of the volcanic rocks. The volcanic belts and basins are arranged (from east to west) as; Kibi-Winneba belt, Cape Coast Basin, Ashanti Belt, Kumasi Basin, Sefwi-Bibiani Belt, Sunyani Basin, Bui Belt, Maluwe Basin and Bole-Nangodi Belt (Fig. 2). The Lawra volcanic belt, located in the northwestern part of Ghana, is the only belt that trends approximately N–S.

The Kibi-Winneba volcanic belt is located towards the southeastern part of Ghana in the West African Craton (Fig. 1) and is characterised by volcanic lobes, made up of basaltic flows, andesitic lavas, pyroclastic and sedimentary rocks, with granitoids occupying intervening positions. This belt displays very similar lithological and structural characteristics to the volcanic belts located in western Ghana.

In comparison to the other volcanic belts, the Kibi-Winneba belt, which is the closest to the Pan African mobile belt, has received very little attention in geochemical studies. Even though this belt displays a wealth of information about petrogenetic evolution and related magmatic processes, only little information on its geochemical and geochronological characteristics has been reported. For these reasons, the petrogenetic relationship between the volcanic belts, the sedimentary basins and granitic intrusions is not well known. In contributing to this, we present high-precision zircon U–Pb geochronological and whole-rock geochemical data for granitoid suites from the Asamankese area of the Kibi-Winneba belt. The aim of this study is to determine the ages of the different types of granitoids and also to provide deeper insight into their petrogenesis and tectonic setting.

2. Geological setting

The Kibi-Asamankese area (Fig. 3), which is a part of the Kibi-Winneba volcanic belt, is made up of basaltic flows, andesitic lavas, amphibolites and pyroclastics, with granite–diorite plutonic suites (Yao and Robb, 1998). Mafic plutonic bodies also intrude this part of the belt. Both Birimian metavolcanics and metasediments of the Kibi area are intruded by different types of granitoids. The granitoids extend from southwest of Asamankese to the west of Suhum and are represented by two-mica granodiorites, biotite granites, hornblende-biotite granite, leucogranites, pegmatoids and migmatites, and gneissic biotite granites (Hirdes et al., 1992).

The biotite granites and granodiorites are grey, medium-grained and foliated, with biotite as their major mafic mineral. The biotite granodiorites are light pink to light grey, equigranular or occasionally porphyritic and foliated. The main mineral constituents are quartz, alkali feldspar, plagioclase and biotite (± hornblende), with minor constituents including pink garnets and greenish chlorites (Hirdes and Davis, 1998). The hornblende granites have intruded the Birimian volcanic rocks near Padi village, on the main Asamankese–Suhum road (Fig. 3). The most obvious feature in all the outcrops is the presence of mafic enclaves, made up mostly of amphibolites and gabbros (Attoh et al., 2006).

Two main suites of granitoids, namely the Dixcove- (or belt-type) and Cape Coast-type (or basin-type) granitoids, intrude the Birimian terrane of the Kibi-Asamankese area (Yao and Robb, 1998). The metaluminous, relatively Na rich, Dixcove-type granitoids, which are dominantly hornblende- to biotite-bearing grano-

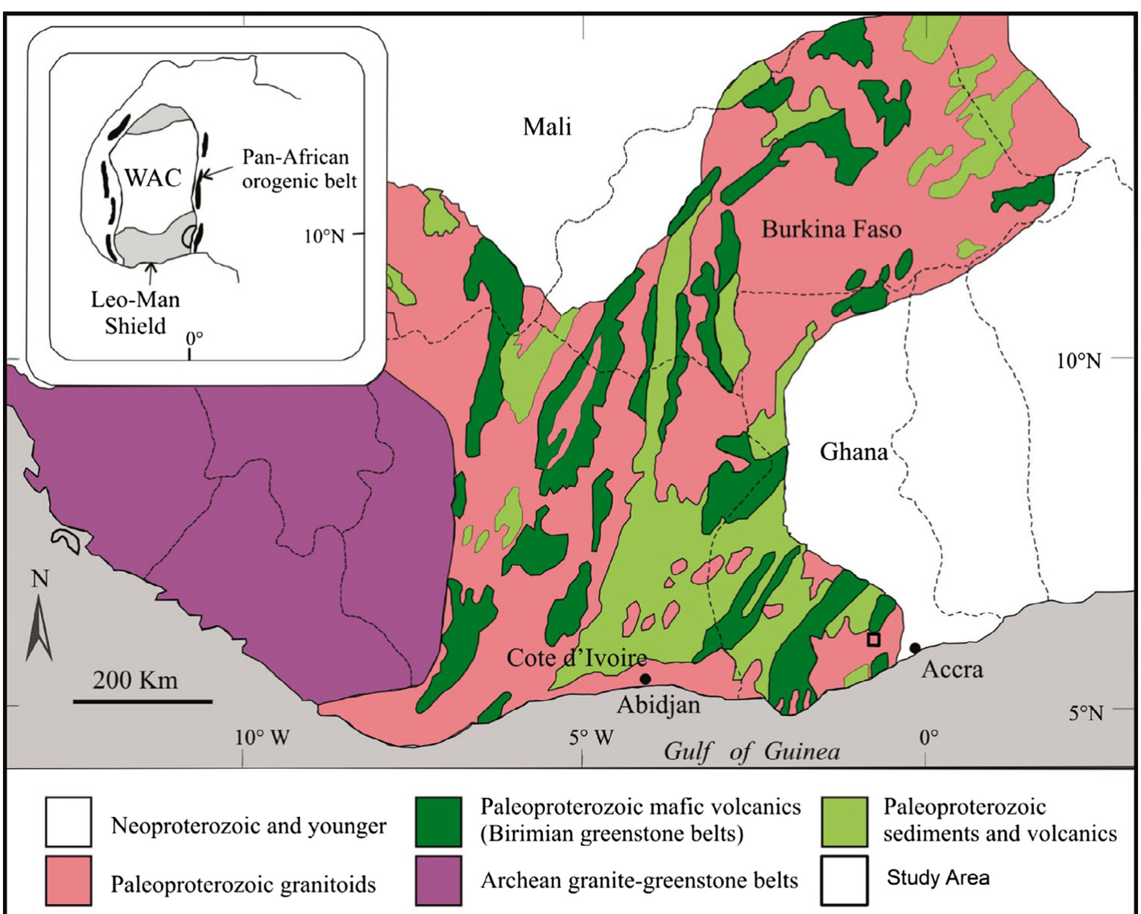

Fig. 1. Simplified geological map of the Man shield showing the West African Craton and Palaeoproterozoic Birimian rocks (Modified after Attoh et al., 2006). The study area is also shown.

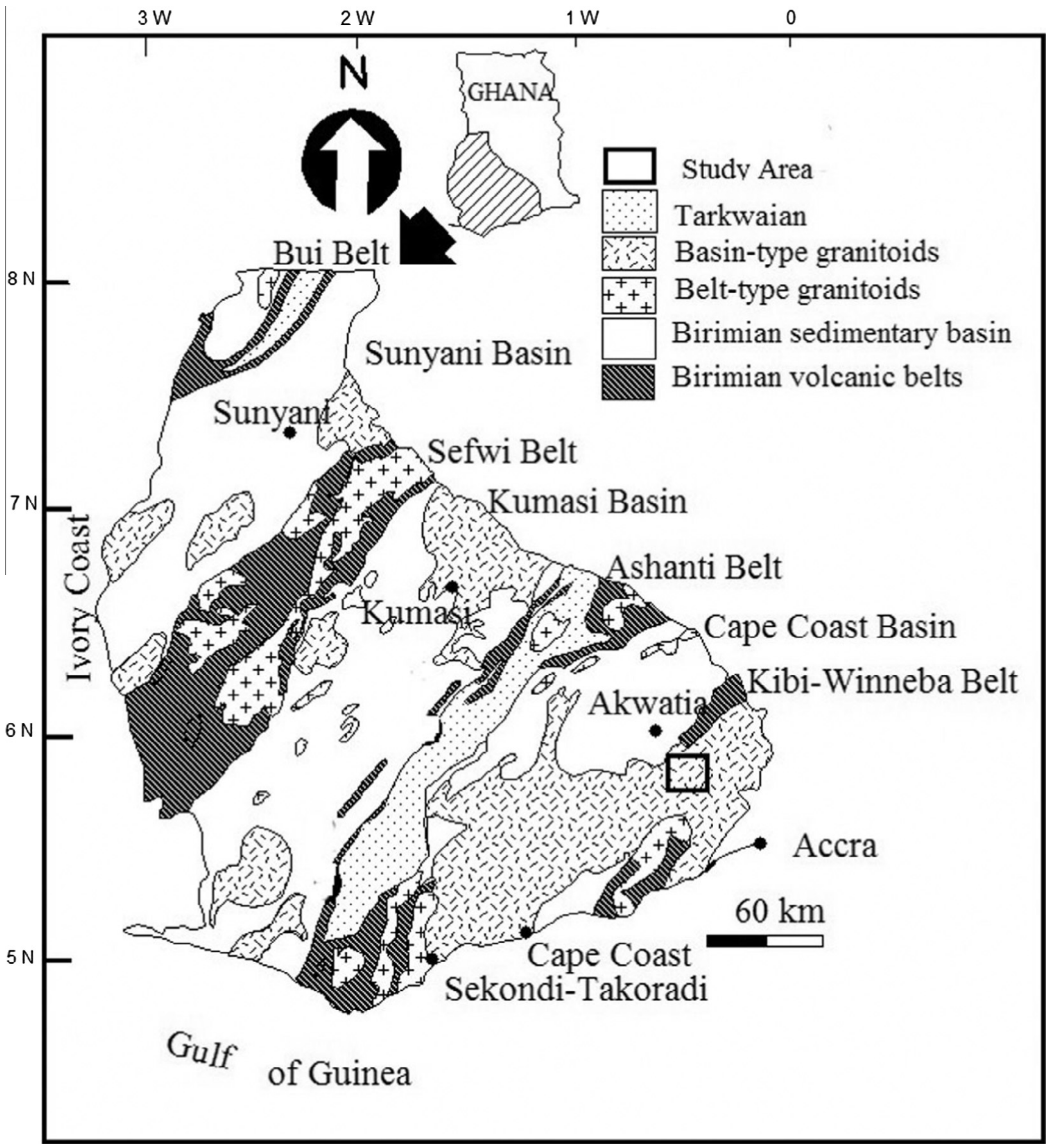

Fig. 2. The geology of southwestern part of Ghana (modified from Leube et al., 1990), showing the study area.

diorite to diorite, monzonite and syenite, intrude the Birimian volcanic belts and they may be coeval with the volcanic rocks (Eisenlohr and Hirdes, 1992). The Cape Coast-type granitoids, which are predominantly peraluminous, two-mica granodiorites, with lesser hornblende- and biotite-bearing granodiorites, are emplaced within the Birimian sedimentary basins. The Dixcove-type granitoids have been dated at 2172 ± 1.4 Ma in the Ashanti Belt (Hirdes et al., 1992) whereas the Cape Coast-type is between 2104 ± 2 and 2123 ± 3 Ma in the Kumasi Basin (Oberthür et al., 1996). Other types of granitoids include the localised, biotite and hornblende granitoids belonging to the Winneba-type, and the K-rich Bongo-type granitoids which cut the Tarkwaian rocks in the volcanic belts. The Cape Coast-, Kumasi-, Dixcove- and Bongo-type granitoids have strong mantle affinities whereas the Winneba-type has an Archean sialic precursor (Sm–Nd model age of ~2.6 Ga) (Taylor et al., 1992), and is believed to be the only rock suite in Ghana which shows such evidence.

The study area lies in the Kibi-Winneba Belt and extends from the Kibi area to the south, and into the adjacent Cape Coast Basin (Figs. 2 and 3). Junner (1943) has extensively described the geology of the Cape Coast Basin. The Birimian Supergroup in the study area is mainly composed of metasedimentary rocks comprising tuffaceous metagraywackes with subordinate quartzites and interbedded grey and black phyllites and schists. Mafic to ultramafic lavas and sub-volcanic rocks are common. In the southern portion of the study area, the metasedimentary rocks are intruded by basin-type granitoids. Other post-Birimian intrusive rocks include granite, aplite, porphyry and pegmatite. The Birimian rocks in the study area generally exhibit up to greenschist facies regional metamorphism (Junner, 1943). Both the metasedimentary rocks and the ultramafic intrusives close to granite batholiths display various degrees of contact metamorphism (Junner, 1943), and they have been affected by low-grade metasomatic alterations, involving silicification and widespread formation of secondary chlorite and sericite. Overlying the Birimian rocks are Pliocene to Recent alluvial deposits.

3. Methodology

Rocks in the study area have experienced various degrees of weathering and alteration, coupled with the scarcity of outcrops.

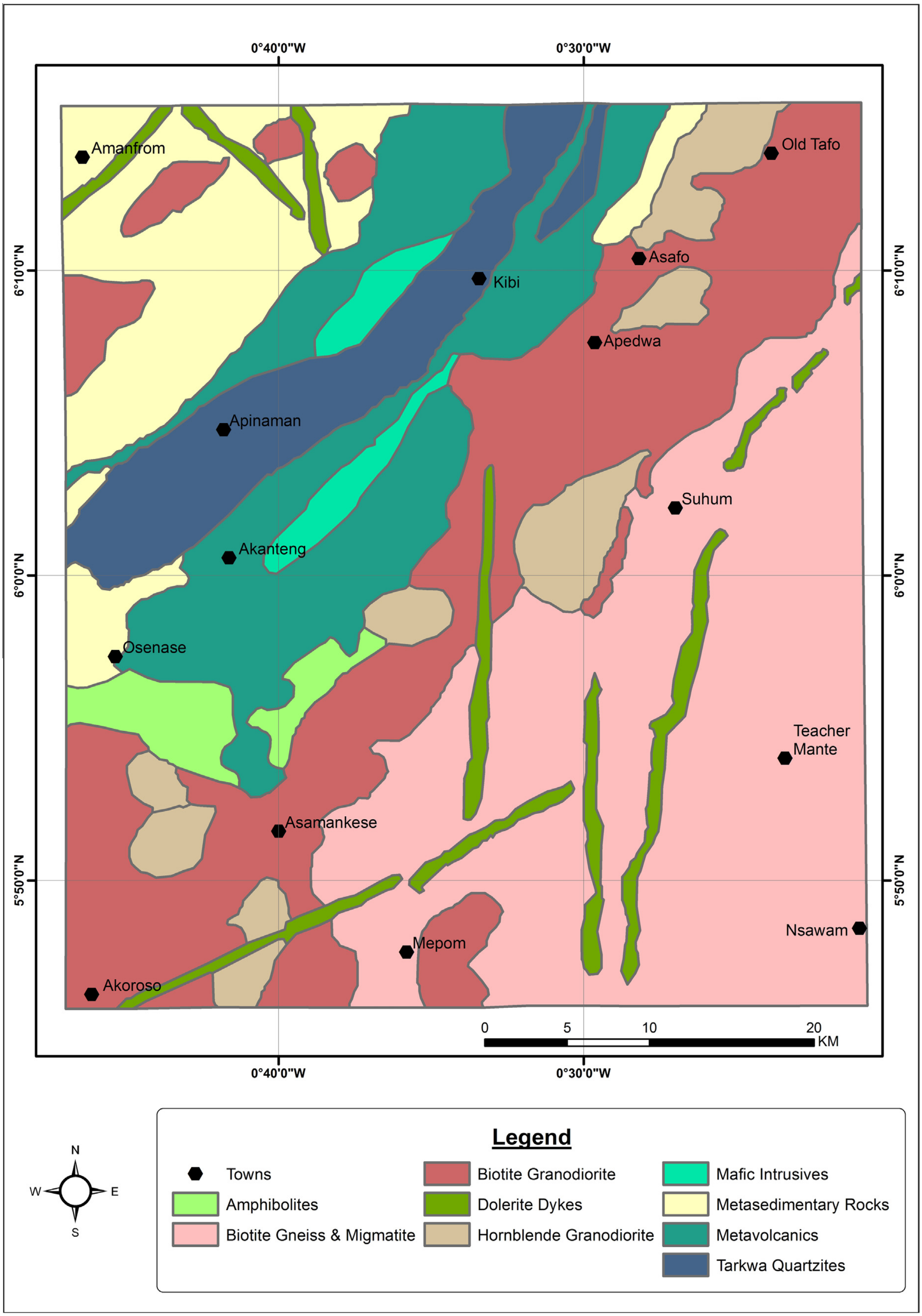

Fig. 3. Geological map of the Kibi-Asamankese area showing the distribution of the various rock units. Modified after Geological Survey Department (2009)

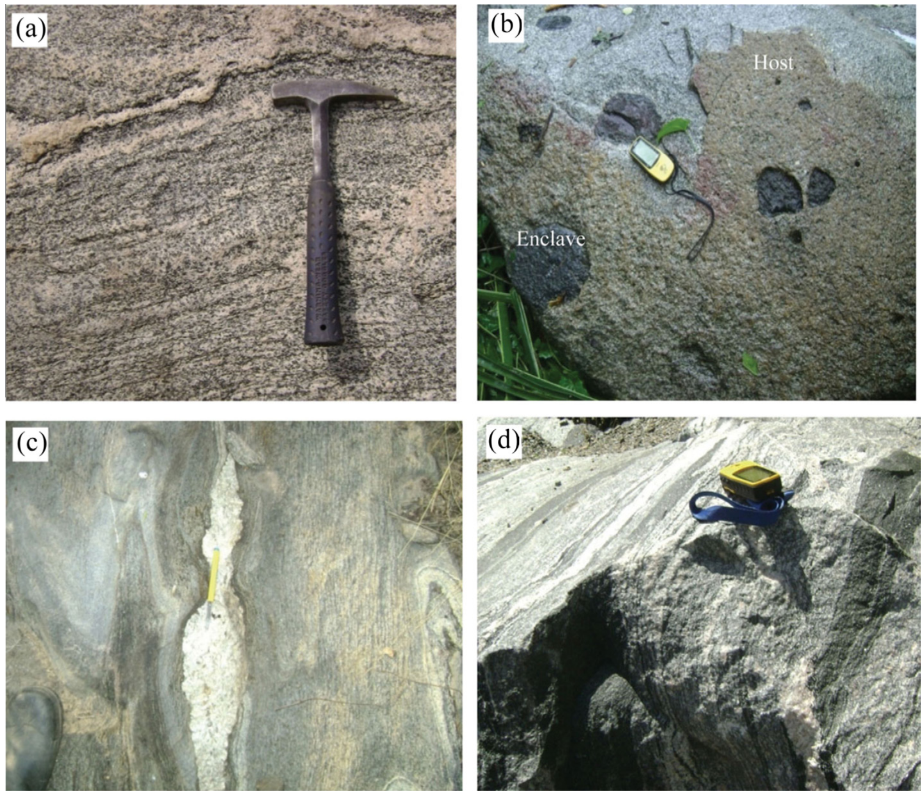

Fig. 4. Outcrop photographs of granitoid rocks in the Asamankese area. (a) Biotite granodiorite; (b) hornblende granodiorite; (c) gneissic biotite granite and (d) gneissic biotite granite.

Of the granitoid samples collected, only the fresh interior of those that were least affected by weathering/alteration were used for the analysis. Accordingly, a total of seven representative samples were selected for analysis. Whole-rock geochemical analysis and U–Pb dating of zircons were performed at the Institute of Geology and Geophysics, Chinese Academy Science (IGGCAS), Beijing, China.

3.1. Major and trace elements

For major elements analysis, chips of whole rock samples free of any weathered surface were crushed and ground in an agate mill to ~200 mesh. Approximately 0.5 g of the rock powder was mixed with ~3–6 g of $Li_2B_4O_7$, and 3–4 drops of NH_4Br was added and the mixture fused in a furnace to form a glass disk. The disks were then analysed using Shimadzu X-ray fluorescence (XRF-1500) with a current and voltage of 50 mA 60 and 50 kV, respectively.

For trace element analysis, about 100 mg of crushed whole-rock powder were dissolved in 2 ml HF and 1 ml HNO_3 in a closed Teflon bomb, which was heated on a hot plate at ~140 °C, then opened and subsequently evaporated to dryness to remove silica. Thereafter, 1.5 ml HF, 1.5 ml HNO_3 and 10 ml $HClO_4$ were added to the Teflon bomb. The bomb was placed in a steel jacket and heated in an oven at 190 °C for 5 days to completely dissolve the sample. This was followed by dry down and addition of concentrated HNO_3 to form nitrates, followed by a final evaporation. Then, 2 ml 50% HNO_3 was added to the Teflon bomb, which was subsequently put into the jacket again and heated to 150 °C for 24 h. Finally, 0.5 g Rh (1 ppm) was added to the solution as an internal standard, and then the solution was diluted by a factor of 500. The solutions were then analysed using ICP-MS. Precisions of the ICP-MS analyses were generally better than 5%. All sample preparations and analyses were performed at the IGGCAS following the procedures described elsewhere (Chu et al., 2009). Analytical uncertainties were 1–3% relative to elements present in concentrations >1 wt.%, and about 10% relative to elements present in concentrations <1 wt.%.

3.2. Zircon U–Pb dating

Zircon grains were separated using conventional heavy fraction and magnetic techniques. Together with zircon standard TEMORA, they were mounted in epoxy and then polished to expose the crystals, possibly halfway, for analysis. Thereafter, all the zircons were photographed in transmitted and reflected lights, and cathodoluminescence (CL) images were obtained to identify and examine the analysed grains. The mounts were then vacuum-coated with high-purity gold. U and Pb isotopes were measured using Cameca IMS 1280 SIMS at the IGGCAS. The measured Pb isotopic compositions were corrected for common Pb using non-radiogenic ^{204}Pb. Corrections were satisfactorily small to be insensitive to the preference for common Pb composition. An average of present-day crustal composition (Stacey and Kramers, 1975; Wiedenbeck et al., 1995) was used for the common Pb. Data reduction was carried out using the Isoplot/Ex rev. 2.49 Program (Ludwig, 2001). Detailed analytical protocols and procedures followed those described in Li et al. (2010).

4. Results

4.1. Field observations and petrography

Based on the mineral assemblages, the studied granitoids from the Kibi-Asamankese area were grouped into three types, namely: biotite granodiorite, hornblende granodiorite and gneissic biotite granites.

4.1.1. Biotite granodiorite

The best exposures of the biotite granodiorites (e.g., S001) occur along the road as isolated hills between Asamankese and Kofi Pare. The granodiorites are generally massive, medium- to coarse-grained and locally deformed (Fig. 4a). They are leucocratic and contain quartzo-feldspathic zones. Weak parallel alignment of felsic and mafic minerals in certain portions, sometimes with abundant biotite and chlorite, define very weak foliation. The major mineral contents are quartz (60–50%), plagioclase (30–25%) K-feldspar (10–5%), and biotite (8–5%). The principal mafic mineral is biotite, but in some samples traces of hornblende are observed.

4.1.2. Hornblende granodiorite

The hornblende granodiorites (e.g., S010b) intrude the Birimian volcanic rock and occur as small sub-rounded plutons. Very good exposures occur near the Padi village, on the main Asamankese–Suhum road. The hornblende granodiorites are massive to weakly foliated. They are light to somewhat dark grey, and medium- to course-grained although they become relatively finer at some locations. The major constituent minerals are quartz (58–50%), plagioclase (35–30%), hornblende (10–5%), and biotite (<2%). Accessory minerals are sphene, zircon, epidote and muscovite. The most common feature in these granitoids is the presence of enclaves of amphibolites and gabbroic rocks. The enclaves vary in shape from large layered to small elongated and slightly rounded bodies (Fig. 4b).

4.1.3. Gneissic biotite granite

The migmatites and gneissic biotite granites occur on the hills north of the town of Adeiso. Typical example is sample S003a. The rocks are coarse- to medium-grained and contain mainly ~65% quartz, K-feldspar (20–15%), plagioclase (10–5%) and biotite (10–5%). Accessory minerals include zircons, sphene and opaque minerals. Gradational sequences of biotite schists, biotite gneisses, and migmatites are seen along the Kua River. Supracrustal xenoliths, derived from the Birimian metasedimentary rocks (e.g., biotite schist), are found within the gneissic biotite granites. The xenoliths are commonly ellipsoidal, occasionally rounded, but are all strongly flattened in the plane of the pervasive foliation, with most of them exhibiting relict layering. Contacts between the xenoliths and the enveloping granodiorite are not always sharp, but sometimes appear gradational. The xenoliths sometimes appear partially absorbed within the granites. The migmatitic zones are characterised by the presence of strongly deformed biotite schists, biotite granites, biotite gneisses, and pegmatites. These zones have common deformational features, including ptygmatic folds and boudins. Almost all the gneissic granites outcrops are cut by pegmatite or aplite dykes and quartz veins and display a weak foliation, which is concordant to the magmatic flow banding (Fig. 4c and d).

4.2. Geochemistry

The major and trace elements results of the studied samples are listed in Table 1. They have high SiO_2 (62.49–69.02 wt.%), Na_2O (2.93–5.14 wt.%), and Al_2O_3 (12.95–14.66 wt.%) contents, with low MgO (0.90–4.22 wt.%) and TiO_2 (0.60–0.74 wt.%) contents (Table 1). SiO_2 defines negative trends against TiO_2, Fe_2O_3T, MgO, and CaO, whereas diffused trends are observed in SiO_2 against Al_2O_3 and P_2O_5 (Fig. 5). On an AFM diagram, the samples display mainly tholeiitic signature with minor contribution from calc-alkaline series (Fig. 6a). Apart from sample S010b which plots in the peraluminous field of the A/CNK–A/NK diagram of Shand (1943) (Fig. 6b), all the remaining samples plot within the metaluminous field with A/CNK compositions ranging between 0.69 and 0.88. The granitoids were classified based on their Ca, Mg, Fe, Ti, and Al composition, after De La Roche et al. (1980). They plot mainly in the fields of granite, granodiorite, diorite, tonalite and trondhjemite (Fig. 6c and d). Almost all the analysed granitoid samples are sodic in composition, with K_2O/Na_2O values ranging from 0.28 to 0.53, with the exception of sample S010b which is potassic in composition ($K_2O/Na_2O \sim 1.3$).

On chondrite-normalised REE diagram, the granitoid samples display fractionated REE patterns, with LREE enrichment and a nearly flat HREE depletion (La_N/Yb_N = 8–79; Yb_N = 1.45–6.56) (Fig. 7a). The rocks show slightly negative to slightly positive Eu

Table 1
Major (wt.%) and trace (ppm) elements of granitoids in the Asamankese area of the Kibi-Winneba belt.

Sample	S001	S010b	S013b	S032	S039
SiO_2	65.27	64.60	62.49	69.02	62.45
Al_2O_3	14.42	14.66	12.95	14.02	12.89
Fe_2O_3T	5.95	7.26	6.54	4.03	7.48
MgO	2.27	2.23	4.22	0.90	4.02
CaO	4.39	1.76	5.07	3.34	4.70
Na_2O	3.81	2.93	4.58	5.14	4.28
K_2O	2.01	3.83	1.83	1.46	2.08
MnO	0.09	0.09	0.12	0.04	0.14
TiO_2	0.70	0.74	0.63	0.60	0.58
P_2O_5	0.22	0.23	0.20	0.19	0.14
LOI	0.80	1.55	1.27	1.16	1.15
Total	99.93	99.88	99.90	99.90	99.91
Li	96	91.2	42.8	127	54.8
Be	1.95	1.78	1.61	1.64	2.43
Sc	10.5	9.06	13.7	3	15.1
V	145	182	128	58.8	169
Cr	46.1	82.3	233	19.9	215
Co	14.8	19.8	23.1	8.01	25.4
Ni	24.6	39.3	113	8.07	147
Cu	21.9	7.34	29.9	7.16	44.9
Zn	94	100	114	134	129
Ga	23.9	23.2	22.6	26.9	23.8
Rb	71	166	68.2	62.2	85.9
Sr	647	136	474	603	431
Y	14.5	7.36	12.9	4.6	11.2
Nb	6.3	10.6	6.53	6.76	3.48
Mo	0.424	0.683	0.157	0.329	0.22
Cd	0.113	0.098	0.162	0.068	0.22
In	0.061	0.074	0.049	0.053	0.059
Sb	0.043	0.073	0.1	0.045	0.066
Cs	7.43	14.5	3.83	8.98	8.12
Ba	840	561	542	591	551
La	29.3	13.8	21.1	35.6	15.7
Ce	56	52.1	41.4	64	30.7
Pr	6.92	2.74	5.46	7.52	3.68
Nd	29.1	11	24.5	31	16.4
Sm	5.06	1.93	4.5	5.07	3.06
Eu	1.71	0.589	1.31	1.29	0.883
Gd	4.15	1.82	3.73	3.35	2.57
Tb	0.627	0.274	0.549	0.375	0.402
Dy	3	1.48	2.76	1.35	1.93
Ho	0.513	0.282	0.462	0.179	0.382
Er	1.45	0.809	1.33	0.391	1.15
Tm	0.231	0.151	0.207	0.046	0.202
Yb	1.37	1.01	1.26	0.304	1.24
Lu	0.201	0.134	0.169	0.034	0.186
Ta	0.423	0.918	0.371	0.406	0.148
W	0.188	1.97	0.064	0.212	0.205
Re	0.009	0.008	0.001	0.00	0.00
Tl	0.446	1.17	0.435	0.378	0.572
Pb	17.7	15.5	14	17.5	10.8
Bi	0.075	0.069	0.131	0.045	0.306
Th	3.94	2.8	2.83	4.07	2.28
U	1.45	1.08	1.68	1.07	1.56
Zr	129	154	137	154	136
Hf	3.57	3.88	3.34	3.73	3.20

Note: Fe_2O_3T = total Fe.

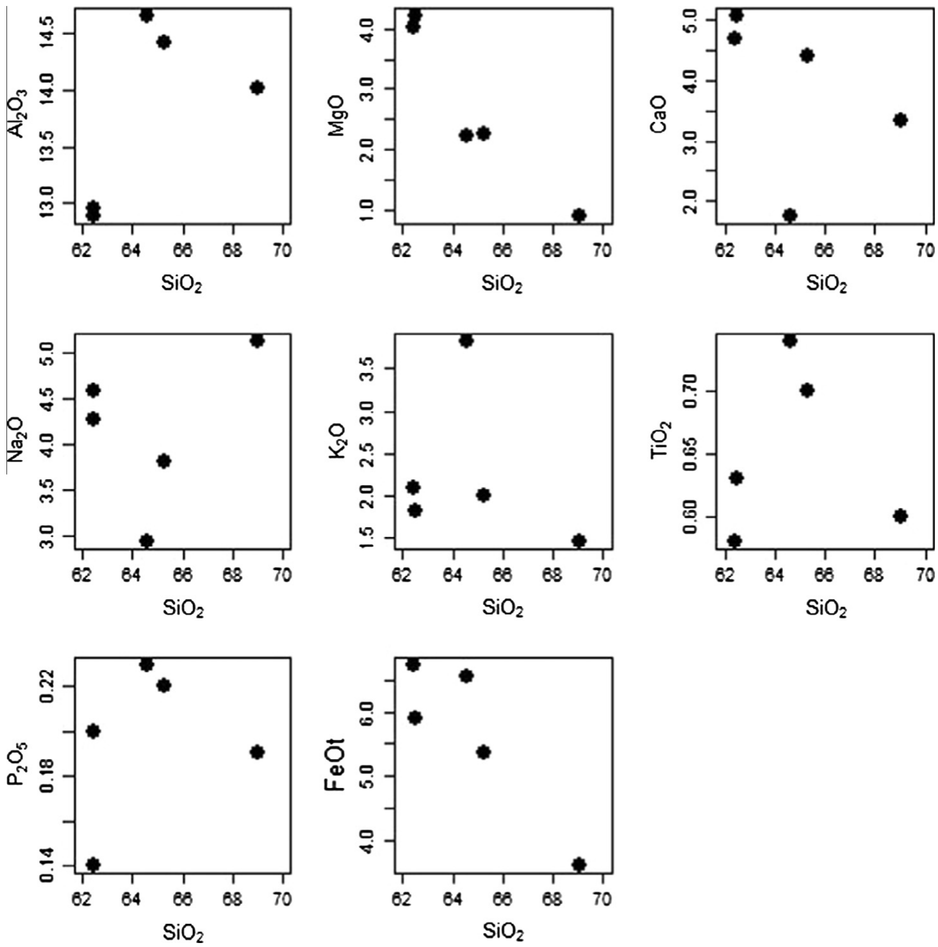

Fig. 5. Harker diagrams of the granitoids in the Kibi-Asamankese area, showing the major elements plotted against SiO_2. Most of the major oxides display negative correlation with SiO_2.

anomalies (Eu/Eu* = 0.98–1.15). On the orogenic granitoid normalised plot (Fig. 7b), the LILE, Th, Ba, and Rb form a bell-shaped curve since K_2O values are less enriched. The HFSE are generally depleted but show small positive Sm and Ce anomalies. In the multi-element spider diagram normalised to primitive mantle (Fig. 7c), the studied granitoids display generally positive Ba, strong negative Nb–Ta, Ti and P anomalies and variable Sr anomalies, generally akin to those of the global average upper crust (e.g., Rudnick and Gao, 2003). Compared with the composition of the lower crust, the studied granitoids are depleted in Ti, P, Sr and Ba, and enriched in U, Th and Rb (Fig. 7d).

4.3. Zircon U–Pb ages

A total of 4 granitoid samples were selected for zircon U–Pb dating. The CL images of representative zircons are shown in Fig. 8. The Kibi-Asamankese granitoids contain anhedral to euhedral, equant to short prismatic zircons. They are generally colourless, transparent to translucent and range in length from 30 to 200 μm, and widths ranging from 25 to 120 μm with aspect ratios of 1.3:1–2.5:1. The equant grains display regular concentric zoning, with bright luminescence, while the short prismatic grains have oscillatory or patchy zonation, with low luminescence; with other grain types having unzoned core and oscillatory zoned rims (Fig. 8). All these features suggest a magmatic origin for the zircon grains. The U–Pb analytical spots for constituent zircon grains ranged from 15 to 20 per studied sample. All of them have very large variations in U and Th contents, with low to moderate Th/U values.

Fifteen zircon grains from sample S001 have large variations in U and Th contents of 128–499 ppm and 31–128 ppm, respectively, and Th/U values of 0.14–0.28, yielding a mean age of 2127 ± 6.7 Ma (MSWD = 1.4) (Table 2; Fig. 9). The U and Th concentrations of fourteen zircon grains from S003a are 69–358 ppm and 32–141 ppm, respectively. They have Th/U values of 0.38–0.59, and a concordia age of 2193.2 ± 8.7 Ma (MSWD = 1.5) (Table 2; Fig. 9). Of the fifteen zircon grains dated from S004, the U and Th contents are 47–1308 ppm and 6–162 ppm respectively, with Th/U values and concordia age of 0.05–0.54 and 2133 ± 13 Ma (MSWD = 2), respectively (Table 2; Fig. 9). The U and Th concentrations of nineteen zircons from S010b are 71–366 ppm and 37–343 ppm, respectively. They have Th/U values of 0.51–1.15, and a concordia age of 2147.8 ± 5.3 Ma (MSWD = 1.06) (Table 2; Fig. 9).

5. Discussion

5.1. Petrogenesis and geotectonic implication

The crustal growth and tectonic development of the Paleoproterozoic Birimian terrane in West Africa has remained the subject of debate over the years. Different ideologies have resulted in the proposal of different models to explain the geotectonic evolution of the West African Craton (WAC). For example, a crustal growth

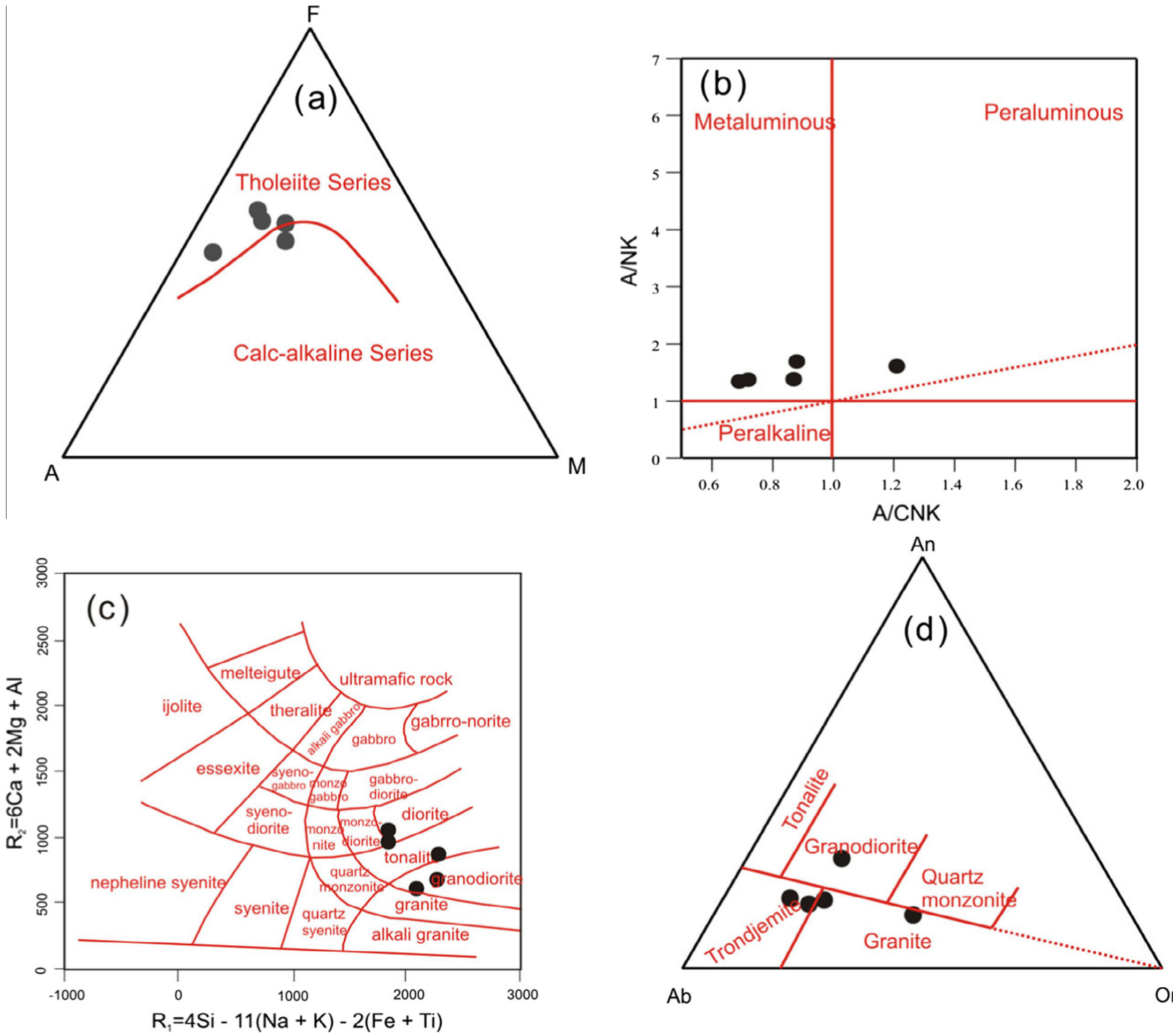

Fig. 6. (a) AFM diagram of the Asamankese granitoids (Irvine and Baragar, 1971). The samples plot mainly within the tholeiitic series; (b) plot of A/NK vs. A/CNK showing metaluminous to weak peraluminous signatures of the Asamankese granitoid rocks (Shand, 1943). (c) Classification of Asamankese granitoids after De la Roche et al. (1980); (d) Ab–An–Or plot of the Asamankese granitoid rocks (Barker, 1979).

mechanism that emphasises on volcanic arc collision and thrusting have been proposed (e.g., Sylvester and Attoh, 1992; Béziat et al., 2000; Feybesse et al., 2006; Pouclet et al., 2006), whereas others argue for Archaean type model with dominant diapirism (e.g., Pons et al., 1995; Vidal et al., 2009).

The moderately high fractionation of REE, producing LREE enrichment and nearly flat HREE depletion (La_N/Yb_N = 8–79) could be attributed to fractionation of plagioclase + hornblende + pyroxene during fractional crystallisation or partial melting at low pressures ($\leqslant$5 kbar) (Lompo, 2009). Therefore the studied rocks were most likely derived from an evolved magma (i.e., magma that has seen much fractionation) or partial melting of the depleted mantle. The granitoid samples from the Kibi-Asamankese area are generally tholeiitic to calc-alkaline in nature, enriched in LILEs such as Cs, K, Rb, U and Th with respect to the HFSEs, especially Nb and Ti. Magmas with such chemical characteristics are generally postulated to have been generated in subduction related environments (e.g. Floyd and Winchester, 1975; Rogers and Hawkesworth, 1989; Sajona et al., 1996).

That notwithstanding, the variable Sr- and Eu-anomalies are indicative of varying extents of plagioclase fractionation since plagioclase has exceptionally high positive Sr and Eu anomalies but depleted in all other REEs and Y (McKay et al., 1994). Similarly, the positive Ba, strong negative Nb–Ta, P and Ti anomalies and variable Sr anomalies displayed by the studied rocks suggest that the sources of the granitoids may be more depleted in HFSE than typical orogenic granitoid. Furthermore, the enrichment in LILE and depletion in HREE and HFSE, coupled with the pronounced negative P–Nb–Ta–Ti anomaly are typical of rocks formed in an arc setting (subduction zone).

Numerous studies (e.g., Pearce et al., 1984) have suggested that trace elements could be used as discriminatory tools to distinguish among different tectonic settings of granitoids. Pearce et al. (1984) used plots of Rb, Y, and Nb elements as the most efficient discriminants amongst ocean-ridge granites (ORG), within-plate granites (WPG), volcanic-arc granites (VAG) and syn-collisional granites (syn-COLG). In the tectonic setting discrimination diagram by Pearce et al. (1984) (Fig. 10) the Kibi-Asamankese granitoids plot mainly in the field defined by volcanic arc granites (VAG), further supporting the argument that the studied granitoids are arc rocks. These VAG belong to the group of "active continental margin" rocks (Pearce et al., 1984). While diagrams such as these do not

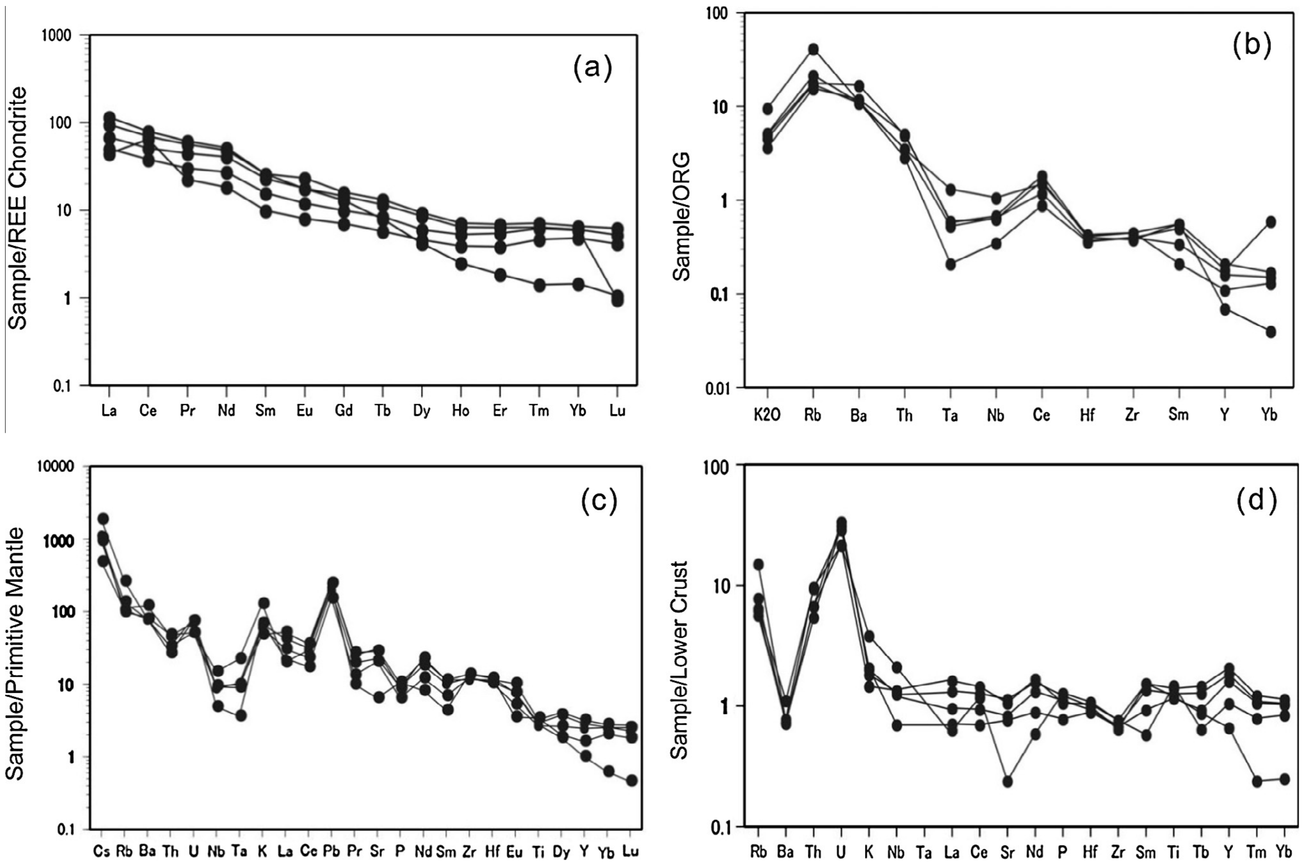

Fig. 7. (a) Chondrite-normalised REE patterns for the Kibi-Asamankese granitoids. Chondrite normalising values are from Boynton (1984). The patterns show enrichments in the LREE and depletion in HREE; (b) trace element spider plot for the granitoids normalised against orogenic granites (after Pearce et al., 1984); (c) primitive mantle-normalised trace elements variation diagrams for the Kibi-Asamankese granitoids. Normalisation factors from Sun and McDonough (1989); (d) spider plots for REE and trace elements for the studied granitoids normalised against Lower Crust (after Weaver and Tarney, 1984).

make a distinction between island or continental arcs, they reinforce the interpretation that emplacement of the granitoids took place in a subduction setting. Further arguments in favour of volcanic arc characteristics of the Kibi-Asamankese granitoids come from their Rb/Zr and Rb/Cs values. All the granitoid samples display low values of Rb/Cs (6.9–11.4) and Rb/Zr (0.55–1.07), which are compatible with volcanic arc settings (Harris et al., 1986).

Even though the granitoids were formed in the same tectonic setting, the differences in, for example, REE-enrichment or ferromagnesian content indicate that they were not formed from the same source. This suggests temporal and/or spatial changes in subduction style. Contamination and mixing were considered in determining the composition of the granitoids. Sample S010b contains basaltic enclaves (Fig. 4b), probably derived from volcanic rocks in the greenstone belts, and therefore the relationship between the enclave and S010b strongly suggests mixing of magmas.

No chemical analysis is available on the basaltic enclave in S010b. However, analyses were carried out on metabasalts and andesites from the Kibi-Winneba belt with which these granitoids are associated, and their REE chondrite-normalised curves vary from LREE enrichment (basalt) to HREE depletion (Anum, 2014). Metavolcanic rocks from the southern Ashanti belt, analysed by Sylvester and Attoh (1992), also show similar patterns.

Trace element compositions of magmas are also dependent on protolith composition and, therefore, may not necessarily be indicative of the tectonic setting of magma formation (e.g. Roberts and Clemens, 1993). However, the spatial and temporal relationships of the Kibi-Asamankese granitoids, in conjunction with their geochemical characteristics indicate a subduction-related origin.

Doumbia et al. (1998) and Gasquet et al. (2003) showed that all their investigated granitoids in the Birimian in Niger, Senegal and Burkina Faso exhibit LILE enrichment relative to the HFSE, with Nb–Ta depression. These patterns are typical of granitoids emplaced in active margins. A contribution from a within-plate type source would have resulted in the enrichment in both Nb and Ta. Therefore the patterns obtained for the studied samples are compatible with granitoids generated in immature island arc or continental arc settings (Brown et al., 1984). The REE plots of granitoids from the Kibi-Asamankese area show LILE enrichment relative to strong Nb–Ta depression (Fig. 7c), which indicates that the granitoids were emplaced in an active margin. Furthermore, the moderately to highly fractionated REEs $(La/Yb)_N$ of the granitoids, with low $(Yb)_N$ values could be ascribed to evolution of a juvenile crust (Lompo, 2009).

The obtained ages (Table 2) in this study allowed the authors to determine the intrusion and extrusion ages of magmatic rocks, the age of their sources and metamorphism, and all these enabled the stratigraphic order of the lithological units and geotectonic processes to be established.

5.2. Implications for Birimian granitoids in Ghana

This study shows that the Kibi-Asamankese area does not differ significantly from the other Birimian domains of the Leo Rise, with respect to the nature and age of emplacement of the granitoids (e.g., Abouchami et al., 1990; Taylor et al., 1992; de Kock et al., 2011; Sakyi et al., 2014). Three generations of granitoids can be recognised in the study area: the first generation is the

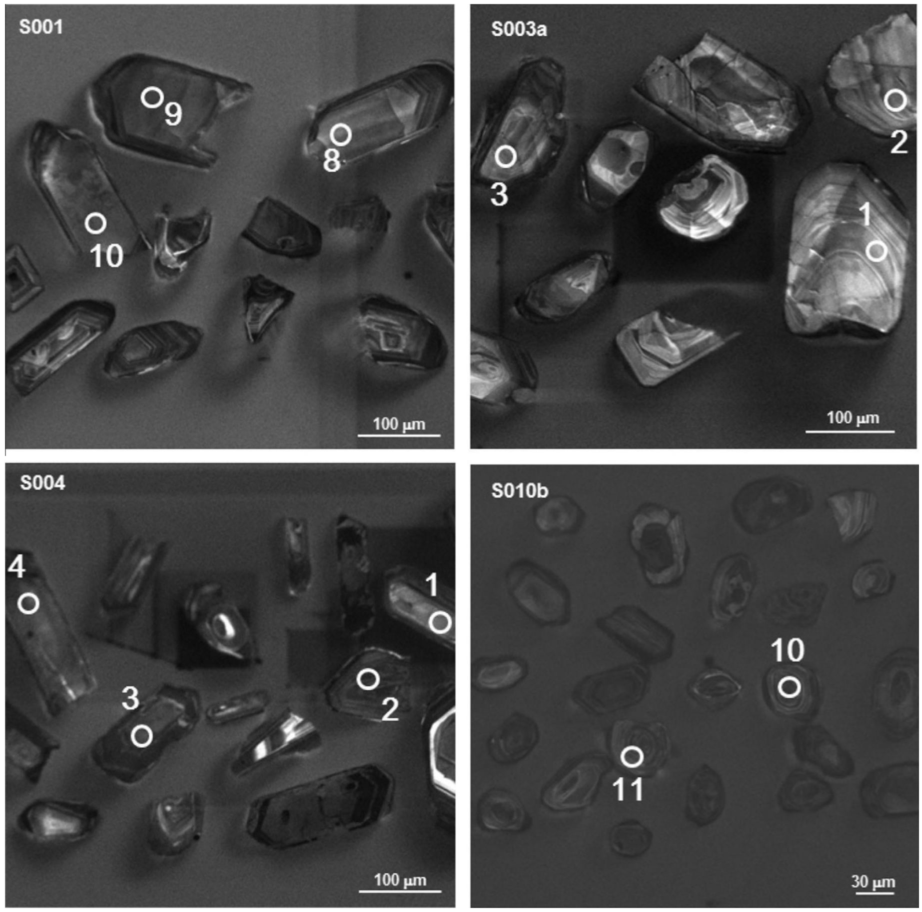

Fig. 8. Cathodoluminescence (CL) images of representative zircons of the studied granitoids rocks from the Asamankese area. Circles indicate SIMS analysed spots for U–Pb isotopes.

Pre-Eburnean gneissic biotite granites emplaced at *ca.* 2193 Ma; the second generation is Eburnean belt type granitoid, *ca.* 2148 Ma and the third generation is the Eburnean basin granitoids, *ca.* 2127 Ma and 2133 Ma. The ages of all the studied rocks fall within the age range (2100–2200 Ma) previously obtained from local and regional studies (Boher et al., 1992; Hirdes et al., 1996; Lüdtke et al., 1999; Hirdes and Davis, 2002).

Biotite granites and granodiorites in the Kibi-Asamankese area form part of the Cape Coast basin granitoid association, with ages of 2133–2127 Ma that are comparable to those of the Sunyani and Kumasi basins (Hirdes et al., 1996). According to Hirdes et al. (1996), the Kumasi basin granitoid sample (2116 ± 2 Ma) is a biotite tonalite, whereas the Sunyani basin granitoid sample (2088 ± 1 Ma) is a muscovite-bearing granitoid, and they gave several possible interpretations accounting for the 30 Ma age difference between these two (late-kinematic) basin granitoid plutons. One possible explanation is the compositional difference between the granitoids in the two basins as indicated above. Such an explanation corroborates the observations of Percival and Sullivan (1988) and Card (1990) in the Superior Province of Canada. These authors describe an age difference of several million years between consanguineous biotite- and muscovite-bearing granitoid intrusions. A second hypothesis would involve a scenario in which contemporaneously formed neighbouring volcanic belts are accreted progressively onto each other. More specifically, in the study area, the Sefwi belt was accreted onto the Ashanti belt prior to the accretion of the Bui belt onto the Sefwi belt. Such a progressive accretion would involve diachronous crustal shortening and deformation, and could trigger the generation of basin granitoid melts. The two differing age dates of 2116 Ma (Kumasi basin) and 2088 Ma (Sunyani basin) would thus represent "docking ages" for the respective neighbouring volcanic belts (Fig. 2). The latter hypothesis would be compatible with structural data recently acquired in Ghana (Eisenlohr and Hirdes, 1992), where accretion would result initially in regional penetrative low-strain deformation, forming S1 foliation. Additional strain related to continuing accretion and crustal shortening would be accommodated subsequently in spatially well-defined and restricted high-strain zones, producing S2 foliation, and these would form preferably at the margins of volcanic belts.

The geochemical signatures of some hornblende granites are comparable to those of typical Archaean TTGs, showing high Na/K ratios and strongly fractionated REE patterns with low Yb contents and a concave shape of their HREE end. Hence, they may have been generated by similar processes. Petrogenetic hypotheses advocated for these granitoids is partial melting of a basaltic protolith metamorphosed to amphibolite facies (e.g., Barker and Arth, 1976; Condie, 1986; Martin, 1987, 1994; Drommund and Defant, 1990). This may be supported by the presence of rocks of mainly basaltic composition and numerous enclaves (Fig. 4b) of basic country rocks (amphibolite) in the study area, which may represent possible remnants of a basaltic crust that could have been partially melted to yield the parental magmas of the hornblende granodiorite. With few exceptions, the studied samples show a high degree of REE fractionation (La_N/Yb_N = 8–79) and HREE depletion (Yb_N = 1.45–6.56), characterised by weak or lack of negative

Table 2
U–Pb isotope data for zircons in granitoids from the Kibi-Asamankese area of the Kibi-Winneba volcanic belt.

Sample/spot #	U (ppm)	Th (ppm)	Pb (ppm)	Th/U	$^{207}Pb/^{235}U$	±σ (%)	$^{206}Pb/^{238}U$	±σ (%)	$^{238}U/^{206}Pb$	±σ (%)	$^{207}Pb/^{206}Pb$	±σ (%)	$t_{207/206}$	±σ	$t_{207/235}$	±σ	$t_{206/238}$	±σ
S001																		
1	235	55	108	0.23	7.00	1.57	0.385	1.50	2.60	1.50	0.132	0.452	2125	7.9	2111	14.0	2098	27.0
2	482	128	194	0.27	5.97	1.57	0.335	1.50	2.98	1.50	0.129	0.462	2086	8.1	1971	13.8	1863	24.3
3	373	71	167	0.19	6.88	1.56	0.379	1.50	2.64	1.50	0.132	0.441	2122	7.7	2096	14.0	2070	26.6
4	164	42	75	0.26	6.97	1.66	0.380	1.51	2.63	1.51	0.133	0.692	2136	12.1	2107	14.8	2078	26.8
5	499	69	214	0.14	6.65	1.54	0.367	1.50	2.73	1.50	0.132	0.344	2119	6.0	2067	13.7	2015	26.0
6	189	43	80	0.23	6.43	1.66	0.352	1.53	2.84	1.53	0.133	0.628	2132	11.0	2036	14.7	1943	25.7
7	285	54	122	0.19	6.52	1.65	0.359	1.58	2.78	1.58	0.132	0.457	2120	8.0	2049	14.6	1979	27.0
8	128	31	59	0.24	6.92	1.61	0.381	1.50	2.62	1.50	0.132	0.581	2118	10.1	2101	14.4	2083	26.8
9	253	54	117	0.21	7.03	1.58	0.388	1.51	2.58	1.51	0.131	0.442	2115	7.7	2115	14.1	2115	27.3
10	186	52	86	0.28	6.94	2.14	0.383	2.08	2.61	2.08	0.131	0.508	2116	8.9	2103	19.2	2090	37.3
11	198	36	91	0.18	7.01	1.74	0.389	1.67	2.57	1.67	0.131	0.483	2108	8.5	2113	15.6	2118	30.3
12	295	56	135	0.19	7.03	1.55	0.386	1.50	2.59	1.50	0.132	0.396	2126	6.9	2116	13.9	2106	27.0
13	177	45	83	0.26	7.10	1.67	0.387	1.56	2.59	1.56	0.133	0.607	2140	10.6	2124	15.0	2107	28.1
14	292	81	125	0.28	6.36	1.58	0.351	1.50	2.85	1.50	0.131	0.489	2114	8.6	2026	14.0	1941	25.2
15	238	62	113	0.26	7.17	1.57	0.393	1.50	2.55	1.50	0.132	0.441	2131	7.7	2133	14.0	2135	27.4
S003a																		
1	99	45	50	0.46	7.69	1.65	0.403	1.51	2.48	1.51	0.138	0.680	2208	11.8	2195	15.0	2181	27.9
2	148	80	76	0.54	7.55	1.60	0.401	1.50	2.49	1.50	0.137	0.555	2183	9.6	2179	14.5	2174	27.8
3	101	44	51	0.44	7.61	1.67	0.400	1.53	2.50	1.53	0.138	0.683	2204	11.8	2186	15.1	2167	28.2
4	94	38	47	0.40	7.52	1.78	0.398	1.50	2.51	1.50	0.137	0.957	2190	16.5	2175	16.1	2160	27.6
5	195	103	97	0.53	7.26	1.60	0.386	1.50	2.59	1.50	0.136	0.560	2181	9.7	2144	14.4	2105	27.0
6	151	61	77	0.40	7.75	1.60	0.406	1.50	2.46	1.50	0.138	0.559	2208	9.7	2202	14.5	2196	28.0
7	75	29	37	0.38	7.57	1.87	0.400	1.55	2.50	1.55	0.138	1.048	2196	18.1	2182	16.9	2167	28.6
8	358	141	137	0.39	5.79	1.56	0.305	1.50	3.28	1.50	0.138	0.429	2198	7.4	1946	13.6	1717	22.7
9	127	48	63	0.38	7.67	1.63	0.400	1.52	2.50	1.52	0.139	0.587	2218	10.1	2193	14.7	2167	28.0
10	69	32	35	0.47	7.40	1.78	0.398	1.51	2.51	1.51	0.135	0.948	2161	16.4	2161	16.1	2161	27.7
11	129	63	66	0.49	7.59	1.61	0.403	1.50	2.48	1.50	0.137	0.590	2184	10.2	2184	14.6	2184	27.9
12	163	73	83	0.45	7.66	1.64	0.404	1.50	2.47	1.50	0.137	0.646	2195	11.2	2192	14.8	2189	28.0
13	146	85	77	0.59	7.63	1.65	0.406	1.51	2.46	1.51	0.136	0.656	2178	11.4	2188	14.9	2198	28.2
14	122	50	61	0.41	7.56	1.66	0.399	1.51	2.50	1.51	0.137	0.689	2194	11.9	2180	15.0	2166	27.8
15	107	49	55	0.45	7.65	1.72	0.406	1.50	2.46	1.50	0.137	0.844	2186	14.6	2191	15.6	2196	28.0
S004																		
1	181	88	86	0.49	6.83	1.60	0.376	1.51	2.66	1.51	0.132	0.522	2121	9.1	2090	14.2	2058	26.6
2	824	81	263	0.10	4.80	1.77	0.277	1.57	3.60	1.57	0.125	0.807	2035	14.2	1785	15.0	1578	22.1
3	236	50	100	0.21	6.41	1.62	0.354	1.50	2.82	1.50	0.131	0.619	2115	10.8	2034	14.4	1955	25.3
5	193	82	94	0.42	7.13	1.58	0.390	1.50	2.56	1.50	0.133	0.493	2133	8.6	2128	14.2	2123	27.2
6	121	25	53	0.21	6.72	1.68	0.373	1.52	2.68	1.52	0.131	0.724	2107	12.6	2075	15.0	2043	26.6
7	242	95	115	0.39	6.97	1.60	0.384	1.50	2.60	1.50	0.131	0.559	2117	9.8	2107	14.3	2097	27.0
8	68	23	31	0.34	6.74	2.37	0.375	1.85	2.67	1.85	0.130	1.485	2102	25.8	2078	21.2	2054	32.6
9	111	45	53	0.40	6.99	1.65	0.383	1.51	2.61	1.51	0.132	0.664	2129	11.6	2110	14.7	2090	26.9
10	297	162	142	0.54	6.88	1.57	0.377	1.50	2.65	1.50	0.132	0.444	2129	7.7	2096	14.0	2062	26.6
11	47	7	22	0.14	7.23	1.86	0.398	1.56	2.51	1.56	0.132	1.009	2121	17.6	2141	16.7	2161	28.8
12	1308	141	375	0.11	4.17	1.66	0.248	1.50	4.03	1.50	0.122	0.714	1983	12.7	1668	13.7	1430	19.3
13	689	100	222	0.14	4.79	1.69	0.277	1.62	3.61	1.62	0.125	0.449	2036	7.9	1783	14.3	1576	22.7
14	112	6	49	0.05	6.92	1.68	0.388	1.50	2.58	1.50	0.129	0.751	2089	13.2	2102	15.0	2115	27.1
15	291	116	135	0.40	6.92	1.60	0.374	1.50	2.68	1.50	0.134	0.546	2154	9.5	2101	14.3	2047	26.4
S010b																		
2	158	157	83	0.99	6.79	1.62	0.373	1.50	2.68	1.50	0.132	0.605	2125	10.6	2085	14.4	2045	26.3
3	165	149	76	0.90	6.09	1.71	0.331	1.51	3.02	1.51	0.133	0.805	2142	14.0	1989	15.1	1845	24.3
4	104	69	51	0.66	6.85	1.66	0.374	1.50	2.68	1.50	0.133	0.705	2137	12.3	2092	14.8	2047	26.4
5	87	62	46	0.71	7.33	1.63	0.395	1.53	2.53	1.53	0.135	0.577	2158	10.0	2152	14.7	2146	27.9
6	130	117	69	0.90	7.06	1.58	0.383	1.50	2.61	1.50	0.134	0.481	2147	8.4	2118	14.1	2089	26.9
7	198	166	97	0.84	6.69	1.57	0.361	1.50	2.77	1.50	0.134	0.454	2156	7.9	2071	14.0	1987	25.8
8	271	273	141	1.01	6.80	1.54	0.369	1.50	2.71	1.50	0.134	0.367	2145	6.4	2086	13.8	2026	26.1
9	366	343	107	0.94	3.98	2.09	0.218	1.90	4.60	1.90	0.133	0.869	2134	15.1	1630	17.1	1269	21.9
10	187	202	107	1.08	7.32	1.55	0.396	1.50	2.53	1.50	0.134	0.397	2152	6.9	2152	14.0	2151	27.5
11	177	139	90	0.79	6.95	1.59	0.375	1.50	2.66	1.50	0.134	0.531	2155	9.2	2105	14.2	2054	26.5
12	206	162	104	0.78	6.83	1.65	0.367	1.54	2.73	1.54	0.135	0.587	2166	10.2	2090	14.7	2013	26.7
13	218	200	113	0.91	6.81	1.58	0.372	1.50	2.69	1.50	0.133	0.495	2134	8.6	2087	14.1	2040	26.3
14	292	236	142	0.81	6.59	1.77	0.356	1.61	2.81	1.61	0.134	0.734	2157	12.8	2059	15.7	1962	27.3
15	344	277	156	0.81	6.12	2.64	0.332	2.13	3.01	2.13	0.133	1.561	2144	27.0	1992	23.3	1850	34.4
16	71	37	29	0.52	5.71	2.83	0.314	1.57	3.19	1.57	0.132	2.354	2123	40.7	1933	24.8	1760	24.3
17	307	213	112	0.69	4.97	1.73	0.268	1.61	3.73	1.61	0.134	0.638	2157	11.1	1814	14.7	1531	21.9
18	253	292	66	1.15	3.63	1.96	0.197	1.67	5.08	1.67	0.134	1.017	2149	17.7	1556	15.7	1158	17.8
19	165	85	83	0.51	7.20	1.60	0.392	1.50	2.55	1.50	0.133	0.567	2142	9.9	2136	14.4	2130	27.3
20	247	278	77	1.13	4.26	1.89	0.233	1.65	4.29	1.65	0.133	0.916	2133	15.9	1686	15.6	1351	20.1

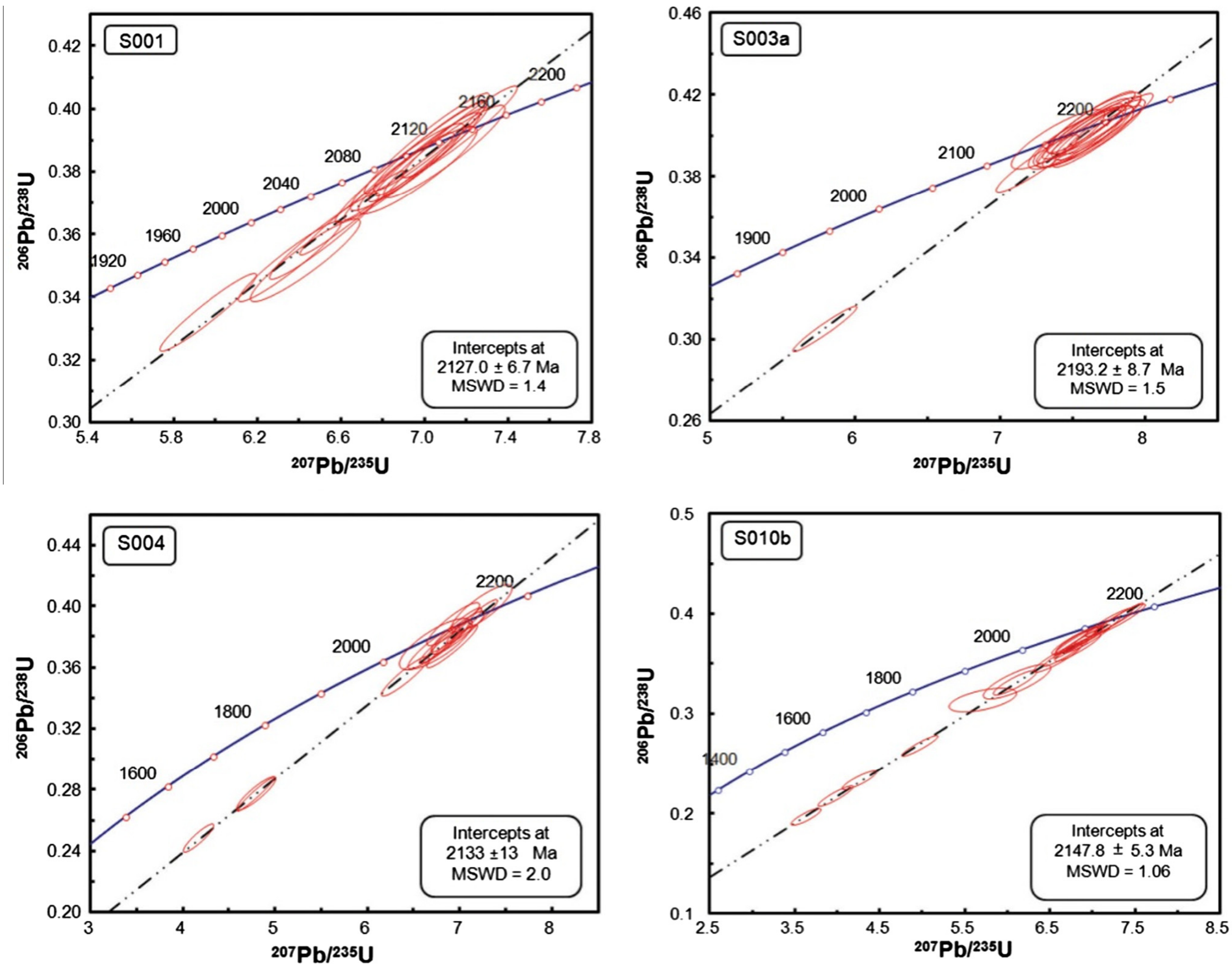

Fig. 9. Zircon U–Pb concordia plots of the studied granitoid rocks from Kibi-Asamankese area of southeastern Ghana.

Eu anomaly. This high degree of fractionation of the REE, as well as the strong HREE depletion and the concave shape of the HREE end could be attributed to the presence of hornblende and garnet as stable constituents of the residue at the site of partial melting (e.g., Martin, 1987, 1994). The negative Nb and Ta anomalies (Fig. 7c) may also support the presence of hornblende in the residue (Drommund and Defant, 1990). Contrary to the discovery of Archaean sialic signature (Sm–Nd model age of ~2600 Ma) in the Winneba granitoid, which suggests that the Birimian is probably underlain by some Archaean basement (e.g., Taylor et al., 1992), the results of this study do not reflect the involvement of Archaean signatures in the formation of the granitoid rocks in the Kibi-Winneba belt and the adjacent Cape Coast basin.

6. Conclusion

The granitoids of the Kibi-Asamankese area are characterised by highly fractionated REE, enrichments in LILE and depletion in Nb, Ta and Sr. REE and trace element chemistry show variation in source rock compositions within single bodies. The enrichment of the LREE and LILE indicates the influence of subduction-related fluids during the melting process in a volcanic arc region, whereas LREE depleted curves indicate sources without fluid enrichment, a typical feature of within-plate regions. Rare earth and trace element ratios indicate that the preferred source of the granitoids was subducted hot oceanic crust with high degree of partial melting.

The field relationships and tectonic events could be placed in sequence for meaningful application of the geochronological data. Foliated and unfoliated metasedimentary, and mafic and granitic enclaves show that the gneissic and foliated granitoids intruded older rock units, some of which had been subjected to earlier tectonism. To differentiate between the various age events, a chronology of events in the study area was established; starting with the basin-forming stage, accompanied by volcanism, sedimentation and finally synchronous plutonism. Deformed metasedimentary enclaves within the Kibi-Asamankese gneissic biotite granites and migmatites are evidence of a pre −2195 Ma tectonism.

The lack of Archaean zircons in the Kibi-Asamankese granitoids, and the presence of abundant cores of Paleoproterozoic ages are indicative of juvenile magmatism, and repeated recycling thereof. The Kibi-Asamankese granitoids comprise several individual granitic intrusions, migmatites and metasedimentary enclaves with the oldest being the gneissic granites dated at 2193.3 ± 8.7 Ma and deformed prior to the succeeding intrusions.

The unfoliated hornblende granodiorite forms part of belt type granitoid that has intruded mainly the Kibi-Winneba metavolcanic rocks from Asamankese to Anum Apapam, and is dated at 2147.8 ± 5.3 Ma. The Kibi-Asamankese biotite granites and

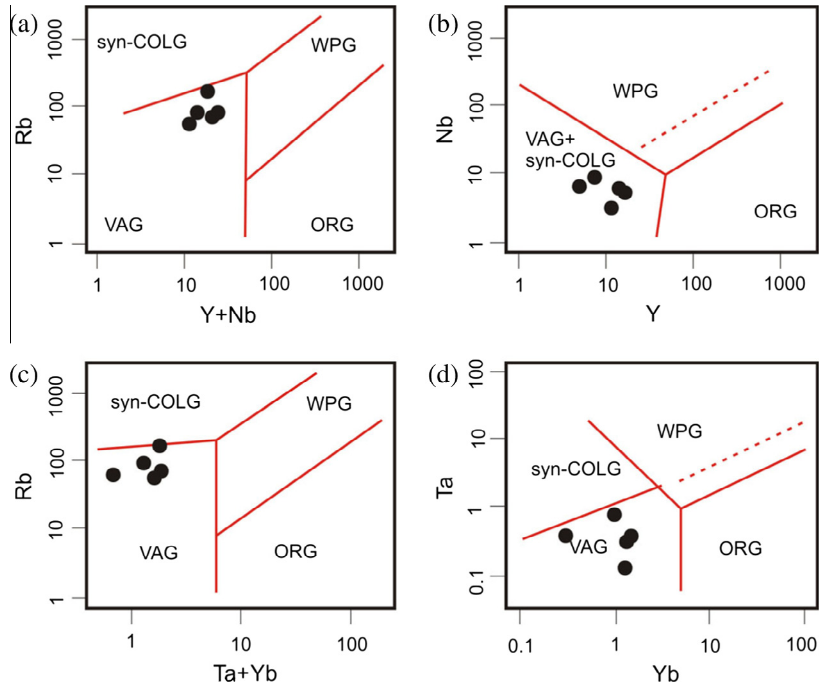

Fig. 10. The discrimination diagrams of geotectonic setting, showing the samples plotting almost exclusively within VAG. (a) Rb vs. Y + Nb (b) Nb vs. Y, (c) Rb vs. Ta + Yb, (d) Ta vs. Yb (Pearce et al., 1984) for the Kibi-Asamankese area granitoid samples. Concentrations of elements are in ppm. Note; WPG: within-plate granite, VAG: volcanic-arc granite, syn-COLG: syn-collisional granite, post-COLG: post-collision granite and ORG: ocean-ridge granite.

granodiorites form part of the Cape Coast basin granitoid association with the Eburnean progeny and have ages between 2127 and 2133 Ma.

Acknowledgements

This research was financially supported by the National Natural Science Foundation of China (Grant 41173011). The paper has benefited from constructive reviews by Pascal Affaton and an anonymous reviewer.

References

Abouchami, W., Boher, M., Michard, A., Albarede, F., 1990. A major 2.1 Ga event of mantle magmatism in West Africa: an early stage of crustal accretion. J. Geophys. Res. 95, 17605–17629.
Anum, S.A., 2014. Geochemistry and Petrology of the Paleoproterozoic Birimian Metavolcanics and Associated Rocks from the Asamankese-Kibi Area in the Eastern Region of Ghana. PhD Thesis, Department of Earth Science, University of Ghana, Legon, 160 pp.
Attoh, K., Evans, M.J., Bickford, M.E., 2006. Geochemistry of an ultramafic-rodingite rock association in the Palaeoproterozoic Dixcove greenstone belt, southwestern Ghana. J. Afr. Earth Sci. 45, 333–346.
Barker, F., 1979. Trondhjemite: definition, environment and hypotheses of origin. In: Barker, F. (Ed.), Trondhjemites, Dacites and Related Rocks. Developments in Petrology, vol. 6. Elsevier, Amsterdam, pp. 1–11.
Barker, F., Arth, J.G., 1976. Generation of trondhjemitic to tonalitic liquids and Archean bimodal trondhjemite-basalt suites. Geology 4, 596–600.
Béziat, D., Bourges, F., Debat, P., Lompo, M., Martin, F., Tollon, F., 2000. A Palaeoproterozoic ultramafic–mafic assemblage and associated volcanic rocks of the Boromo greenstone belt: fractionates originating from island-arc volcanic activity in the West African Craton. Precambr. Res. 101, 25–47.
Boher, M., Abouchami, W., Michard, A., Albaréde, F., Arndt, N.T., 1992. Crustal growth in West Africa at 2.1 Ga. J. Geophys. Res. 97, 345–369.
Boynton, W.V., 1984. Cosmochemistry or the rare earth elements: meteorite studies. In: Henderson, P. (Ed.), Rare Earth Element Geochemistry. Elsevier, Amsterdam, pp. 63–114.
Brown, C.G., Thorpe, R.S., Webb, P.C., 1984. The geochemical characteristics of granitoids in contrasting arcs and comments on magma sources. J. Geol. Soc. (London) 141, 411–426.
Card, K.C., 1990. A review of the Superior Province of the Canadian Shield, a production of Archean accretion. Precambr. Res. 48, 99–156.
Chu, Z.Y., Wu, F.Y., Walker, R.J., Rudnick, R.L., Pitcher, L., Puchtel, I.S., Yang, Y.H., Wilde, S.A., 2009. Temporal evolution of the lithospheric mantle beneath the eastern North China Craton. J. Petrol. 50, 1857–1898.
Condie, K.C., 1986. Origin and early growth rate of continents. Precambr. Res. 32, 261–278.
de Kock, G.S., Armstrong, R.A., Siegfried, H.P., Thomas, E., 2011. Geochronology of the Birimian Supergroup of the West African Craton in the Wa-Bolé region of west-central Ghana: implications for the stratigraphic framework. Geological Society of Africa Presidential Review No. 18. J. Afr. Earth Sci. 59, 1–40.
De La Roche, H., Leterrier, J., Grandclaude, P., Marchal, M., 1980. A classification of volcanic and plutonic rocks using R1R2-diagram and major element analyses – its relationships with current nomenclature. Chem. Geol. 29, 183–210.
Debat, P., Nikiema, S., Mercier, A., Lompo, M., Beziat, D., Bourges, F., Roddaz, M., Salvi, S., Tollon, F., Wenmenga, U., 2003. A new metamorphic constraint for the Eburnean orogeny from Paleoproterozoic formations of the Man shield (Aribinda and Tampelga countries, Burkina Faso). Precambr. Res. 123, 47–65.
Doumbia, S., Pouclet, A., Kouamelan, A., Peucat, J.J., Vidal, M., Delor, C., 1998. Petrogenesis of juvenile-type Birimian (Palaeoproterozoic) granitoids in Central Côte d'Ivoire, West Africa: geochemistry and geochronology. Precambr. Res. 87, 33–63.
Drommund, M.S., Defant, M.J., 1990. A model for trondhjemite–tonalite–dacite genesis and crustal growth via slab melting: Archean to modern comparisons. J. Geophys. Res. 95, 21503–21521.
Eisenlohr, B., Hirdes, W., 1992. The structural development of the early Proterozoic Birimian and Tarkwaian rocks of southwest Ghana, West Africa. J. Afr. Earth Sci. 14, 313–325.
Feybesse, J.L., Billa, M., Guerrot, C., Duguey, E., Lescuyer, J.L., Milési, J.P., Bouchot, V., 2006. The Paleoproterozoic Ghanaian province: geodynamic model and ore controls, including regional stress modelling. Precambr. Res. 149, 149–196.
Floyd, P.A., Winchester, J.A., 1975. Magma type and tectonic setting discrimination using immobile elements. Earth Planet. Sci. Lett. 27, 211–218.
Gasquet, D., Barbey, P., Adou, M., Paquette, J.L., 2003. Structure, Sr–Nd isotope geochemistry and zircon U–Pb geochronology of the granitoids of the Dabakala area (Côte d'Ivoire): evidence for a 2.3 Ga crustal growth event in the Paleoproterozoic of West Africa? Precambr. Res. 127, 329–354.
Geological Survey Department, 2009. Geological map of Ghana 1:1000000.Ghana Geological Survey and Bundesanstalt für Geowissenschaften und Rohstoffe. Geological Survey Department of Ghana, Accra, Ghana.
Harris, N.B.W., Pearce, J.A., Tindle, A.G., 1986. Geochemical characteristics of collision-zone magmatism. In: Coward, M.P., Ries, A.C. (Eds.), Collision Tectonics. Geological Society of London, Special Publication 19, pp. 67–81.
Hirdes, W., Davis, D.W., 1998. First U–Pb zircon age of extrusive volcanism in the Birimian Supergroup of Ghana, West Africa. J. Afr. Earth Sci. 27, 291–294.
Hirdes, W., Davis, D.W., 2002. U–Pb geochronology of Paleoproterozoic rocks in the part of the Kedougou-Kéniéba inlier, Senegal, West Africa: evidence for diachronous accretionary development of the Eburnean Province. Precambr. Res. 118, 83–99.

Hirdes, W., Davis, D.W., Eisenlohr, B.N., 1992. Reassessment of Proterozoic granitoid ages in Ghana on the basis of U–Pb zircon and monazite dating. Precambr. Res. 56, 89–96.

Hirdes, W., Davis, D.W., Lüdtke, G., Konan, G., 1996. Two generations of Birimian (Palaeoproterozoic) volcanic belts in north eastern Côte d'Ivoire (West Africa), as demonstrated by precise U–Pb mineral dating: consequences for 'Birimian controversy'. Precambr. Res. 80, 173–199.

Irvine, T.N., Baragar, W.R.A., 1971. A guide to chemical classification of the common volcanic rocks. Can. J. Earth Sci. 8, 523–548.

Junner, N.R., 1940. Geology of the Gold Coast and Western Togoland. Gold Coast Geological Survey Bulletin, No. 11, p. 40.

Junner, N.R., 1943. The Diamond Deposits of the Gold Coast with Notes on Other Diamond Deposits in West Africa. Gold Coast Geological Survey Bulletin, No. 12, 55 pp.

Leube, A., Hirdes, W., Mauer, R., Kesse, G.O., 1990. The early Proterozoic Birimian Supergroup of Ghana and some aspects of its associated gold mineralization. Precambr. Res. 46, 139–165.

Li, J.Z., Wu, X.Z., Qi, X.F., Zhang, M., Zhang, Q.C., 2010. Distribution and tectonic setting of upper Paleozoic volcanic rock in northern Xinjiang. Acta Petrol. Sin. 26, 195–206 (in Chinese with English abstract).

Lompo, M., 2009. Geodynamic evolution of the 2.25–2.0 Ga Paleoproterozoic magmatic rocks in the Man-Leo Shield of the West African Craton. A model of subsidence of an oceanic plateau. Geological Society, London, Special Publications 323, pp. 231–254.

Lüdtke, G., Hirdes, W., Konan, G., Koné, Y., N'da, D., Traoré, Y., Zamblé, Z., 1999. Géologie de la région Haute Comoé Sud-feuilles Dabakala (2b, d et 4b, d), Direction de la Géologie Abidjan Bulletin, p. 176.

Ludwig, K.R., 2001. User's Manual for Isoplot/Ex rev. 2.49: Berkeley, California. Berkeley Geochronology Centre Special Publication, No. 1a, 56 p.

Martin, H., 1987. Petrogenesis of Archean trondhjemites, tonalities and granodiorites from eastern Finland: major and trace elements geochemistry. J. Petrol. 28, 921–953.

Martin, H., 1994. The Archean grey gneiss and the genesis of continental crust. In: Condie, K.C. (Ed.), The Archean Crustal Evolution. Elsevier, Amsterdam, pp. 205–259.

McKay, G., Le, L., Wagstaff, J., Crozaz, G., 1994. Experimental partitioning of rare earth elements and strontium: constraints on petrogenesis and redox conditions during crystallization of Antarctic angrite Lewis Cliff 86010. Geochim. Cosmochim. Acta 58, 2911–2919.

Oberthür, T., Schmidt Mumm, A., Vetter, U., Simon, K., Amanor, J.A., 1996. Gold mineralization in the Ashanti belt of Ghana: genetic constraints of stable isotope geochemistry. Econ. Geol. 91, 289–301.

Pearce, J.A., Harris, N.B., Tindle, A.G., 1984. Trace element discrimination diagrams for the tectonic interpretation of granitic rocks. J. Petrol. 25, 956–983.

Percival, J.A., Sullivan, R.W., 1988. Age Constraints on the Evolution of the Quetico Belt, Superior Province, Canada. Geological Survey of Canada, Paper 88-2, pp. 97–108.

Pons, J., Barbey, P., Dupuis, D., Leger, J.M., 1995. Mechanisms of pluton emplacement and structural evolution of a 2.1 Ga juvenile continental crust: the Birimian of southwestern Niger. Precambr. Res. 70, 281–301.

Pouclet, A., Doumbia, S., Vidal, M., 2006. Geodynamic setting of the Birimian volcanism in central Ivory Coast (western Africa) and its place in the Paleoproterozoic evolution of the Man Shield. Bull. Soc. Geol. Fr. 167, 529–541.

Roberts, M.P., Clemens, J.D., 1993. Origin of high-potassium, calcalkaline, I-type granitoids. Geology 21, 825–828.

Rogers, G., Hawkesworth, C.J., 1989. A geochemical traverse across the North Chilean Andes: evidence for crust generation from the mantle wedge. Earth Planet. Sci. Lett. 91, 271–285.

Rudnick, R., Gao, S., 2003. Composition of the continental crust. Treatise Geochem. 3, 1–64.

Sajona, F.G., Maury, R.C., Bellon, H., Cotton, J., Defant, M., 1996. High field strength element enrichment of Pliocene–Pleistocene island arc basalts, Zamboanga peninsula, western Mindanao (Philippines). J. Petrol. 37, 693–726.

Sakyi, P.A., Su, B.X., Anum, S., Kwayisi, D., Dampare, S.B., Anani, C.Y., Nude, P.M., 2014. New zircon U–Pb ages for erratic emplacement of 2213–2130 Ma Paleoproterozoic calc-alkaline I-type granitoid rocks in the Lawra Volcanic Belt of northwestern Ghana, West Africa. Precambr. Res. 254, 149–168.

Shand, S.J., 1943. Eruptive Rocks: Their Genesis, Composition, Classification and their Relations to Ore Deposits, second ed. Wiley, New York, 444 pp.

Stacey, J.S., Kramers, J.D., 1975. Approximation of terrestrial lead isotope evolution by a two-stage model. Earth Planet. Sci. Lett. 26, 207–221.

Sun, S.S., McDonough, W.F., 1989. Chemical and isotopic systematics of oceanic basalts: implication for mantle composition and processes. In: Saunders, A.D., Norry, M.J. (Eds.), Magmatism in Ocean Basins, vol. 42. Geological Society of London Special Publication, pp. 313–345.

Sylvester, P.J., Attoh, K., 1992. Lithostratigraphy and composition of 2.1 Greenstone belts of the West African Craton and their bearing on crustal evolution and Archean–Proterozoic boundary. J. Geol. 100, 377–393.

Taylor, P.N., Moorbath, S., Leube, A., Hirdes, W., 1988. Geochronology and crustal evolution of Early Proterozoic granite-greenstone terrains in Ghana/West Africa. In: Abstract, International Conference on the Geology of Ghana with Special Emphasis on Gold. 75th Anniversary of Ghana Geol. Survey Department, Accra, pp. 43–45.

Taylor, P.N., Moorbath, S., Leube, A., Hirdes, W., 1992. Early Proterozoic crustal evolution in the Birimian of Ghana: constraints from geochronology and isotope geochemistry. Precambr. Res. 56, 97–111.

Vidal, M., Alric, G., 1994. The Palaeoproterozoic (Birimian) of Haute-Comoéin the West African Craton, Ivory Coast: a transtensional back-arc basin. Precambr. Res. 65, 207–229.

Vidal, M., Gumiaux, C., Cagnard, F., Pouclet, A., Ouattara, G., Pichon, M., 2009. Evolution of a Paleoproterozoic "weak type" orogeny in the West African Craton (Ivory Coast). Tectonophysics 477, 145–159.

Weaver, B.L., Tarney, J., 1984. Empirical approach to estimating the composition of the continental crust. Nature 310, 575–577.

Wiedenbeck, M., Alle, P., Corfu, F., Griffin, W.L., Meier, M., Oberli, F., Vonquadt, A., Roddick, J.C., Speigel, W., 1995. Three natural zircon standards for U–Th–Pb, Lu–Hf, trace-element and REE analyses. Geostand. Newsl. 19, 1–23.

Yao, Y., Robb, L.J., 1998. The Birimian Granitoids of Ghana: A Review. Information Circular 322. University of the Witwatersrand, Economic Geology Research Unit, Johannesburg, 46 pp.